to dihydrofolate reductase weighs against (iii) above (unless an initial sequestration were followed by delivery to the cell cytoplasm). Likewise, the ineffectiveness of hyperthermia in promoting uptake of free MTX by the tumor (see Fig. 3) indicates that we are not seeing the results of (iv), a heat-induced increase in cellular transport of MTX. Also, increased blood flow (ii) would not be effective in these experiments since uptake of MTX into Lewis lung tumor cells is limited by membrane transport, not by blood flow (*11*).

The more than fourfold ratio of deliveries is itself potentially useful in therapy, and we have no reason to doubt that higher ratios can be obtained by appropriately optimizing the liposome preparation with respect to size, composition, and charge; by optimizing the temperature of heating; and by combining local hyperthermia with generalized hypothermia to increase the available temperature range. As indicated by other experiments in which the lipid was labeled with [^{14}C]DPPC (*22*), it may also be possible to include lipophilic drugs for selective effects analogous to those seen with the water-soluble MTX.

The major limitation of this approach for cancer chemotherapy is that it does not deal with the problem of widely metastatic disease [unless the reported regression of metastases after heating of primary tumors (*23*) turns out to be a useful phenomenon]. In that limitation it is similar to radiotherapy and to local hyperthermia itself. This approach might, of course, be applied to local lymph nodes in the area of a tumor, to other diseases of better-defined localization (for example, infections), or to widespread diseases of the skin (such as psoriasis), in which heating is feasible and systemic drugs such as MTX are sometimes useful (*24*).

J. N. WEINSTEIN
Laboratory of Theoretical Biology, National Cancer Institute, National Institutes of Health, Bethesda, Maryland 20014

R. L. MAGIN*
Laboratory of Chemical Pharmacology, Division of Cancer Treatment, National Cancer Institute

M. B. YATVIN
Radiobiology Research Laboratory, Department of Human Oncology, University of Wisconsin, Madison 53706

D. S. ZAHARKO
Laboratory of Chemical Pharmacology, Division of Cancer Treatment, National Cancer Institute

References and Notes

1. M. B. Yatvin, J. N. Weinstein, W. H. Dennis, R. Blumenthal, *Science* **202**, 1290 (1978).
2. R. E. Pagano and J. N. Weinstein, *Annu. Rev. Biophys. Bioeng.* **7**, 435 (1978); D. Papahadjopoulos, Ed., *Ann. N.Y. Acad. Sci.* **308** (1978).
3. C. Streffer, Ed., *Cancer Therapy by Hyperthermia and Radiation* (Urban & Schwarzenberg, Baltimore, 1978).
4. B. C. Giovanella, *Recent Results Cancer Res.* **59**, 36 (1977).
5. G. M. Hahn, J. Braun, I. Har-Kedar, *Proc. Natl. Acad. Sci. U.S.A.* **72**, 937 (1975).
6. J. T. Leith, R. C. Miller, E. W. Gerner, M. L. M. Boone, *Cancer* **39**, 766 (1977).
7. Increased release of solutes near the transition temperature in vitro has been described by M. C. Blok, L. L. M. van Deenen, J. de Gier, J. A. F. Op den Kamp, and A. J. Verkleij [*FEBS Symp. 42* (1977), p. 38], D. Papahadjopoulos, K. Jacobson, S. Nir, and T. Isac [*Biochim. Biophys. Acta* **311**, 330 (1973)], K. Inoue [*ibid.* **339**, 390 (1974)], and C. M. W. Haest, J. de Gier, G. A. van Es, A. J. Verkleij, and L. L. M. van Deenen [*ibid.* **288**, 43 (1972)].
8. Lipoprotein-induced release from fluid-phase liposomes has been studied by J. Zborowski, F. Roerdink, and G. Scherphof [*Biochim. Biophys. Acta* **497**, 183 (1977)] and G. Scherphof, F. Roerdink, M. Waite and J. Parks (*ibid.*, in press). We find that very high, high, intermediate, and low density human lipoproteins, as well as the density 1.21 g/cm^3 bottom fraction of standard centrifugations, all cause considerable release of liposome contents at the phase transition.
9. W. C. Werkheiser, *J. Biol. Chem.* **236**, 888 (1961).
10. K. H. Yang *et al. (11)*; R. L. Dedrick, D. S. Zaharko, R. J. Lutz, *J. Pharm. Sci.* **62**, 882 (1973); H. K. Kimelberg, *Biochim. Biophys. Acta* **448**, 531 (1976); M. J. Kosloski *et al.*, *Cancer Res.* **38**, 2848 (1978).
11. K. H. Yang, W. P. Fund, R. J. Lutz, R. L. Dedrick, D. S. Zaharko, *J. Pharm. Sci.*, in press.
12. V. T. Oliverio, *Anal. Chem.* **33**, 263 (1961). The procedure was modified in that a volatile buffer, NH_4HCO_3, was used as eluant.
13. The lipid was initially dried from 2 ml of benzene (with a drop of ethanol added) onto the walls of a glass vial, first with a stream of argon gas and then by several hours on a freeze-drying apparatus. Sonication was done under argon in a closed polystyrene container, using a bath sonicator (Laboratory Supplies, Inc., Hicksville, N.Y.). Less leakage was found below transition if a base other than HCO_3^- was used to titrate MTX.
14. Small unilamellar vesicles are metastable below T_c, and they change into larger forms of a different physical chemical nature [J. Suurkuusk, B. R. Lentz, Y. Barenholz, R. L. Biltonen, T. E. Thompson, *Biochemistry* **15**, 1393 (1976)].
15. This technique has been described in (*1*) and, in more detail, in J. N. Weinstein, S. Yoshikami, P. Henkart, R. Blumenthal, and W. A. Hagins [*Science* **195**, 489 (1977)] and J. N. Weinstein, R. Blumenthal, S. O. Sharrow, and P. A. Henkart [*Biochim. Biophys. Acta* **509**, 272 (1978)]. The fluorescence self-quenching approach was developed by Hagins and Yoshikami.
16. Tumors were passed and handled as in protocol 1.400 [R. I. Geran, N. H. Greenberg, M. M. MacDonald, A. M. Schumacher, B. J. Abbott, *Cancer Chemother. Rep. Part 3* **3**, 13 (1972)].
17. R. L. Magin, *IEEE Trans. Microwave Theory Tech.* **27**, 78 (1979).
18. H. K. Kimelberg and M. L. Atchison, *Ann. N.Y. Acad. Sci.* **308**, 395 (1978).
19. Uptake of ^{3}H by liver and kidneys was affected surprisingly little by encapsulation or heating; splenic uptake was much greater with liposomes, as expected; accumulation in muscle, which has little or no dihydrofolate reductase (*10*), was so low as probably to be accounted for by extracellular MTX.
20. J. L. Wisnicki, W. P. Tong, D. B. Ludlum, *Cancer Treat. Rep.* **62**, 529 (1978). This protocol separates MTX from such potential products as 6-methylpteridine, 10-methylpteroate, methylaminobenzoate, and 7-hydroxy-MTX. Recoveries of ^{3}H after processing and elution were generally greater than 90 percent.
21. When we tried to assess the role of the phase transition by injecting MTX in liposomes made with DSPC alone, the average heated/unheated ratio was 2.0 ± 0.2 (standard error, 12 mice). But interpretation of the results was difficult: blood levels of encapsulated MTX were still high after 4 hours (liposomes presumably more stable in the circulation); the T_c of liposomes remaining in the serum after 1 hour was found to have decreased toward 42°C (because of slow interaction with serum components); and little of the MTX appeared to be intracellular.
22. When the lipid of DPPC-DSPC liposomes was labeled with [^{14}C]DPPC, heated/unheated ratios averaged 1.9 ± 0.2 (standard error, 11 mice), considerably smaller than that for MTX. This could be explained in a number of ways: direct interaction between liposomes and cells (fusion, endocytosis, or lipid exchange); metabolic alteration of the DPPC (labeled in the fatty acid chains) and uptake in a different form; or disruption of liposomes by serum components and incorporation of the lipid molecules by a secondary process.
23. S. A Shah and J. A. Dickson, *Cancer Res.* **38**, 3523 (1978).
24. G. D. Weinstein and P. Frost, *Natl. Cancer Inst. Monogr.* **30**, 225 (1969).
25. We thank W. Embry and A. Feister for fine technical assistance and S. Sieber and R. Cysyk for generous provision of space and equipment. We also thank M. Berman, R. Adamson, R. Cysyk, B. Bunow, L. Leserman, R. Blumenthal, R. Parker, P. J. Weinstein, K. Hartman, and A. J. B. M. van Renswoude for critical reading of the manuscript.
* Permanent address: Department of Radiation Biology and Biophysics, School of Medicine and Dentistry, University of Rochester, Rochester, N.Y. 14627.

20 December 1978

X-ray Absorption Edge Fine Structure of Potassium Ions in Various Environments: Application to Frog Blood Cells

Abstract. *The edge spectrum is a sensitive probe of local chemistry. Edge spectra of potassium in various chemical environments were measured, and each environment gives a unique edge spectrum. Hydrated potassium has a unique spectrum that is insensitive to counterions. Comparison of the spectra shows that the chemical state of potassium in cells differs appreciably from that in aqueous solutions.*

Diffusible ions play an important role in resting and action potentials, bioenergetics, and other cellular functions. It is therefore of interest to determine their chemical state in the cell. The central question in past investigations on this subject has been whether the majority of intracellular diffusible ions exist in a state of dilute solution (*1*, *2*). Intracellular ions are called free if their chemical state is similar to that in a water solution at equivalent ionic strengths; otherwise they are regarded as bound. The chemical potentials of free and bound ions are expected to be different. Consequently, the thermodynamics of cellu-

0036-8075/79/0413-0191$00.50/0

lar functions depends on the chemical state of diffusible ions (*3*).

Methods used in the past include electron microscopy, electron probe microanalysis, ion-selective microelectrodes, ion influx and efflux measurements, and nuclear magnetic resonance (*1*, *2*, *4*). Edzes and Berendsen (*1*) concluded that the diffusible ions in cells are essentially free. Because the living cell is a heterogeneous system and the molecular structures within a cell are not known in detail, interpretations of data are not always straightforward. Nonetheless, we were surprised by our experimental finding that the x-ray absorption edge fine structure of potassium in frog blood cells is qualitatively different from that of free potassium in solution. The deviation seems to indicate that the potassium ions are appreciably influenced by intracellular molecules other than water.

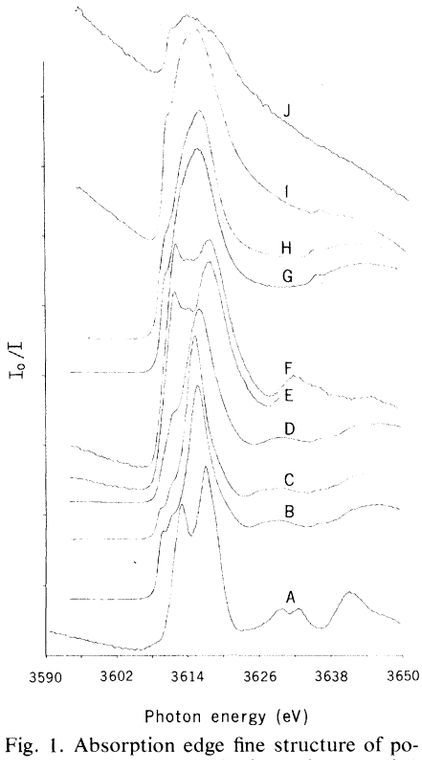

Fig. 1. Absorption edge fine structure of potassiums, plotted as I_0/I (in arbitrary units) versus photon energy. Spectra: (*A*) Crystalline $KTaO_3$ (for the rest of the samples the counterion of K^+ is acetate, unless specified otherwise); (*B*) crystalline K^+-cryptate complex; (*C*) 2*M* K^+-cryptate complex in acetone; (*D*) 2*M* K^+–18 crown 6 complex in ethanol; (*E*) 0.4*M* K^+-valinomycin complex in ethanol; (*F*) 0.4*M* K^+-valinomycin complex in methanol; (*G*) 2*M* potassium acetate in water; (*H*) 2*M* KCl in water; (*I*) 0.2*M* K^+ aqueous solution (75 percent KCl, 15 percent KH_2PO_4, $7\frac{1}{2}$ percent K_2HPO_4); and (*J*) blood cells of leopard frog (*Rana pipiens pipiens*, Schreber). In these displays the vertical scale has been offset for clarity; the absolute value varies considerably from *A* to *J*. It is the relative edge structure that is of interest.

However, lacking further quantitative knowledge about this "unfree" nature, we are not able to estimate the ratio of bound to free ions, if there are indeed simply two such phases.

The importance of our finding stems from the fact that the near-edge structure is a direct measurement of the atomic state of the absorbing element. The spectrum near an absorption edge represents the electronic excited states of the absorbing atom under the influence of its neighbors. We studied the excited states of the K-shell electron from potassium in various chemical environments, including potassium compounds in solid form, potassium-ionophore complexes in solutions, solutions of salts of potassium, and frog blood cells. Aside from the blood cells, the samples were chosen with the knowledge that the nearest neighbor shells of the potassium are composed of oxygen in each case. X-ray transmission spectroscopy experiments were performed at the Stanford Synchrotron Radiation Laboratory (SSRL), using the facility of EXAFS Beamline II. The monochromatized incident x-ray beam, diffracted off a matched pair of Si (111) crystals, had a resolution of about 1.5 eV. The intensity of the incident beam, I_0, and that of the transmitted beam, I, were measured with ion chambers. We used a mixture of He and N_2 in the I_0 chamber and pure N_2 in the I chamber. Helium pathways were used to eliminate x-ray absorption by air. Liquid samples were examined in a specially designed holder (*5*) in which the sample thickness was adjustable and the x-ray beam passed through a total thickness of about 2 mils (0.002 inch) of polyethylene. The absorption edge fine structures of potassium in the samples are expressed in terms of I_0/I in Fig. 1 in the range of photon energy from 3594 to 3650 eV (*6*) (the K edge of potassium is at 3607 eV).

Since oxygen is electronegative, the oxygen nearest neighbor shell presents a potential barrier to the ejected photoelectron in the absorption process. We expect the pre-edge structure to be dependent not only on the radius of the oxygen shell but also on the charge distribution in the shell. However, because of the first-shell barrier, the pre-edge structure should be relatively insensitive to the chemistry beyond the first-shell atoms. Thus the pre-edge structure is a sensitive probe of local chemistry. Spectra *A* to *I* in Fig. 1 demonstrate this sensitivity in a sequence of oxygen environments with varying degrees of structural flexibility, ranging from a rigid crystalline arrangement (*A*) to much more fluid hydration shells (*G* to *I*). Between these two extremes are the oxygen cages of ionophores (*B* to *F*). Since for each sample the spectrum is a statistical average (at room temperature), the most regular and rigid shell (crystal) gives the sharpest spectrum, as one would expect. The hydration shells have the least regular and rigid structure and consequently give rise to the most smeared spectrum: a largely featureless peak except for a shoulder at ~ 3610 eV. Among the ionophores, cryptate has the most rigid oxygen cage, so here the spectra of crystal (*B*) and solution (*C*) are nearly the same. Compared to cryptate, 18 crown 6 has a relatively open or flat structure with the K^+ more exposed to solvent, and this seems to broaden the main peak (at ~ 3617 eV). Valinomycin has an approximately octahedral oxygen cage, so its spectrum is similar to $KTaO_3$ which is a cubic crystal (*7*). In addition, valinomycin is a much more deformable or flexible molecule than cryptate, and therefore the oxygen cage is much more susceptible to perturbation through the nature of the surrounding solution. This is seen in the difference between the spectra *E* and *F*. Indeed, for these two samples the free energies of binding K^+ differ by 3.45×10^{-2} eV, not including the difference due to the solubilities of K^+ in ethanol and methanol (*8*).

We now examine the frog blood cells and aqueous solutions more closely. The 0.2*M* solution (spectrum *I* in Fig. 1) was prepared to roughly simulate the important diffusible ions in cells. The difference in slope before the edge, expecially noticeable in *I* and *J*, is due to the enhanced absorption of the non-

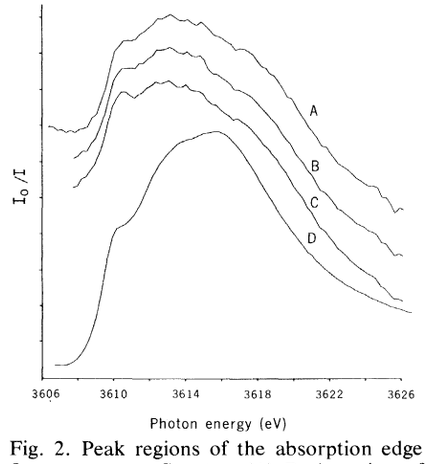

Fig. 2. Peak regions of the absorption edge fine structures. Spectra: (*A*) Peak region of spectrum *J* (blood cells) in Fig. 1, where the measuring time per data point was 10 seconds; (*B* and *C*) same spectrum with better statistics, 30 and 50 seconds per data point, respectively; and (*D*) peak region of spectrum *I* (dilute aqueous solution) in Fig. 1.

potassium part of the solution (background) compared with the potassium contribution. In fact, the slight difference between I and G or H in the peak region and in the height of the shoulder compared to that of the peak is mainly due to this difference in background. Thus spectra G, H, and I provide a measure of the uniqueness of the purely aqueous environment. The near-edge spectrum of hydrated potassium is insensitive to both counterion and potassium concentration.

This uniqueness makes it meaningful to compare the spectrum of the cells with that of the aqueous solution. Figure 2 shows magnified spectra in the peak region, 3608 to 3626 eV. In the blood sample, more than 95 percent of the potassium ions are intracellular. The intracellular potassium concentration is between 0.1 and 0.2M. Spectrum A in Fig. 2 is the peak region of J in Fig. 1. The measuring time for each data point on J in Fig. 1 was 10 seconds. Spectra B and C in Fig. 2 are the same spectrum with better statistics—30 and 50 seconds per point, respectively. One can see that certain features of the potassium spectrum of blood cells are not statistical fluctuations, and that they are qualitatively different from the features of the spectrum of free potassium at a similar concentration, D in Fig. 2. In particular, the height of the low-energy peak at ~ 3610 eV relative to the broad second peak is quite different between the two. The broad peak of the blood cells is shifted to lower energy and is broader, possibly indicating a greater heterogeneity of the K^+ environment than in H_2O. Because the K^+ environments we examined appear fairly unique and distinguishable from one another, we conclude that the differences represented in Fig. 2 are characteristic of the complex binding of K^+ in these frog blood cells and that, for potassium, the cell cannot be regarded as an aqueous solution.

H. W. HUANG
Department of Physics, Rice University, Houston, Texas 77001
S. H. HUNTER
W. K. WARBURTON
Stanford Synchrotron Radiation Laboratory, Stanford, California 94305
S. C. MOSS
Department of Physics, University of Houston, Houston, Texas 77002

References and Notes

1. T. Edzes and H. J. C. Berendsen, *Annu. Rev. Biophys. Bioeng.* **4**, 265 (1975).
2. G. N. Ling and M. M. Ochsenfeld, *J. Gen. Physiol.* **49**, 819 (1966).
3. G. N. Ling, *A Physical Theory of the Living State* (Blaisdell, Waltham, Mass., 1962).
4. C. C. Ashley, in *Membrane and Ion Transport*, E. E. Bittar, Ed. (Wiley-Interscience, New York, 1970), vol. 2, pp. 1–31.
5. S. C. Moss, H. Metzger, M. Eisner, H. W. Huang, S. H. Hunter, *Rev. Sci. Instrum.*, in press.
6. The monochromator was calibrated at the Cu edge (8980 eV). At the potassium edge the scale could be off by a few electron volts.
7. We have tentatively assigned the first peak to the 4*s* vibronic state, and the second peak to the allowed 4*p* state.
8. Stability constants for valinomycin complexes were from W. Simon, W. E. Morf, P. Ch. Meier, *Struct. Bonding (Berlin)* **16**, 114 (1973). Solubilities of K^+ were from H. Stephen and T. Stephen, Eds., *Solubilities of Inorganic and Organic Compounds* (Macmillan, New York, 1963).
9. We thank G. N. Ling for the blood cell samples and SSRL for their hospitality and assistance. Supported in part by ONR contracts N00014-77-C-0239 and N00014-76-C-0273 (to Rice University), PHS grant GM 21721 from the National Institute of General Medical Sciences (Rice University), and the Robert A. Welch Foundation (Rice University and the University of Houston).

8 January 1979

Seaweed Dermatitis: Structure of Lyngbyatoxin A

Abstract. *A highly inflammatory and vesicatory substance, lyngbyatoxin A, has been isolated from the lipid extract of a Hawaiian shallow-water variety of* Lyngbya majuscula *Gomont; its gross structure was determined from chemical and spectral data. Lyngbyatoxin A is closely related to teleocidin B, a poisonous substance associated with several strains of* Streptomyces.

The blue-green alga *Lyngbya majuscula* Gomont is responsible for a severe erythematous, papulovesicular dermatitis known as "swimmers' itch" in Hawaii (*1*, *2*). Since all subjects who come into direct contact with the noxious strains of this cyanophyte develop erythema, followed by blisters and deep desquamation, the active principle is a primary irritant and not an allergen (*2*, *3*). Debromoaplysiatoxin, a poisonous substance that is present (*4*) in a deep-water variety of *L. majuscula* from Enewetak (*5*) and in dermatitis-producing *L. majuscula* from Laie Bay, Oahu (*6*), produces an erythematous pustular folliculitis in humans (*7*) and could be the causative agent of the dermatitis. Not all strains of toxic *L. majuscula*, however, contain debromoaplysiatoxin or its congeners. For example, a toxic shallow-water variety of *L. majuscula* from Kahala Beach, Oahu, contains a different compound, lyngbyatoxin A, which is also a highly inflammatory and vesicatory agent. The structure determination of lyngbyatoxin A, which may represent the first indole alkaloid from a marine plant, is the subject of this report.

Freeze-dried *L. majuscula* from Kahala Beach, Oahu, was extracted successively with petroleum ether and dichloromethane. Gel filtration of the dichloromethane extract on Sephadex LH-20 (*8*) followed by high-pressure liquid chromatography of the toxic fraction on μ-Bondapak-CN with a mixture of hexane and diisopropyl ether (1:1) gave lyngbyatoxin A as a tan gummy solid in 0.02 percent yield.

High-resolution mass spectrometry established the molecular formula of lyngbyatoxin A as $C_{27}H_{39}N_3O_2$ (found: *m/e* 437.3019) and the ^{13}C nuclear magnetic resonance (NMR) spectrum (Table 1) confirmed that 27 carbon atoms were present in the molecule. The ultraviolet spectrum of the toxin in ethanol, which showed bands at 212 (ϵ 18,200), 231 (26,300), 287 (8,900), and 301 nm (9,300), was typical of an indole. A positive Ehrlich test supported the presence of this moiety and also suggested that the C-2 position of the indole was unsubstituted. The ^1H NMR spectrum (Table 1) (*9*) indicated that the indole was trisubstituted as it exhibited a broad singlet at δ 8.50 for the indole NH, a broad singlet at δ 6.81 for the C-2 proton, and two sharp doublets (J = 8 Hz) at δ 6.44 and 6.96 assigned to two vicinal protons on either C-4 and C-5, C-5 and C-6, or C-6 and C-7.

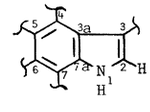

a

Further inspection of the ^1H NMR spectrum revealed doublets at δ 0.62 and 0.89 for secondary methyl groups, a doublet at δ 4.33 for a methine proton, a multiplet at δ 2.55 for a methine proton that was strongly coupled to all three signals at δ 0.62, 0.89, and 4.33, and a singlet at δ 2.87 for an *N*-methyl group of an *N*-methylvaline unit (**b**) (*10*). The amino acid, however, could not be liberated on vigorous acid hydrolysis. The carbonyl in **b** had to be connected to a nitrogen since the ^{13}C NMR spectrum had only one carbonyl carbon signal (δ 174.7) and the infrared spectrum indicated that it was in an amide group (1650 cm^{-1}). The N-13 nitrogen in **b** was therefore attached to the rest of the molecule by a bond that could not be cleaved by acid hydrolysis. This nitrogen also was very weakly basic as the toxin could not be

0036-8075/79/0413-0193$00.50/0